JOURNAL OF AERONAUTICAL MATERIALS
ISSN: 1005-5053

Vol. 44, Issue-01, 2024
pp. 203-222

THE IMPACT OF MILD STEEL, STAINLESS STEEL, AND HIGH-DENSITY POLYETHYLENE ON THE FOAMING ABILITY AND FOAM STABILITY OF AQUEOUS FILM FORMING FOAM IN AVIATION

Nhlanhla F. Khanyi[1], Pavel Y. Tabakov[2], Freddie L. Inambao[3*]

[1]MSc student, Department of Mechanical Engineering, Durban University of Technology (DUT), South Africa.

[2,] Professor, Department of Mechanical Engineering, Durban University of Technology (DUT), South Africa.

[3]* Professor, Department of Mechanical Engineering, University of KwaZulu-Natal Durban 4041, South Africa

*https://orcid.org/0000-0001-9922-5434

*https://scholar.google.com/citations?user=FeBH9xQAAAAJ

*https://www.scopus.com/authid/detail.uri?authorId=55596483700

ABSTRACT

Aqueous Film Forming Foam (AFFF) has become a critical component within the aviation industry. However, relatively few reports address the causes of the poor performance of AFFF during fire conditions due to the rarity of air crashes. Herein, the impact of mild steel, stainless steel, and high-density polyethylene on the foaming ability and foam stability of AFFF was experimentally investigated. The functional groups, particle shape, size, size distribution, and elementary analysis were conducted using the Fourier transform infrared spectroscopy, transmission electron microscopy, dynamic light scattering, and inductively coupled plasma atomic emission spectroscopy. The results showed that all three materials affect the foam ability and foam stability of AFFF in some manner, with mild steel having the most severe impact. The recommendations to use cross-linked polyethylene and fiberglass materials for better storing AFFF concentrate were thoroughly discussed.

Keywords Aqueous film forming foam, foaming ability, foam stability, cross-linked polyethylene, fiberglass.

1 Introduction

Fire protection is a critical sector within any aviation industry, which has created divergent opinions in terms of compliance standards. Aircraft accidents are devastating, considering the loss of lives and costly equipment that must be expected. In aviation, firefighting foam, particularly aqueous film-forming foam (AFFF), is the sole optimum extinguishing agent for the suppression of combustible or flammable liquids.[1] Aviation accidents involving aircraft have dramatically decreased over the past decades and are therefore not a threatening issue. Nonetheless, the aviation industry must adhere to the relevant compliance standards and be fully equipped in case of any unexpected circumstances.

Periodic training is mandatory in all aspects of aviation fire protection in ensuring that firefighting skills and resources within the sector adhere to the Federal Aviation Administration (FAA), National Aviation Authority (NAA), and National Fire Protection Association (NFPA) compliance standards, to react rapidly during accidents. Consequently, periodic testing of the

performance parameters of fire extinguishing foam is a necessity. Unexpected circumstances often happen during periodic tests when AFFF is unable to perform as anticipated. The main priority of AFFF is to suppress the fire and allow possible victims more time to escape during the accident. However, according to relevant compliance standards, all of this must be accomplished in one minute or less upon arrival at the accident scene. The poor performance of AFFF is caused by numerous and diverse factors; hence, it becomes difficult to examine where the problem originates. In past decades, there have been fatal fire accidents in the aviation industry (globally), which has tasked researchers to investigate further the fire protection sector. Nevertheless, there are still notable gaps in previous research conducted, with limited studies on the impact of the materials used to construct the storage tank for storing AFFF concentrate. This is due to the nature and diversity of these problems.[2-4] The complexity of enhancing the firefighting foam in the storage tank construction materials has always been a concern due to the complicated branches of engineering such as material sciences and thermal engineering involved.

In 1965, Meldrum et al.[5] published their study on the storage life and utility of mechanical firefighting foam liquids. The study contributed to predicting the period in which firefighting foams can be held in a storage tank before they deteriorate. Furthermore, it emphasized the gaps and limitations within previous research and the difficulties in problem optimization. The predictions are governed by parameters such as extreme temperatures, oxidation, evaporation, corrosion, dilution, and contamination in the storage tank. Most of this research work is benchmarked in the above study.

This research work has great significance in terms of evaluating and experimentally investigating the impact of mild steel, stainless steel, and high-density polyethylene (HDPE) on the foaming ability and foam stability of AFFF. All manufacturers of firefighting foam concentrate have strict recommendations for storing their products, with the priority being to store the foam concentrate in its original storage tank[6-8]. The challenge arises due to critical factors that must be taken into consideration and often result in large storage tanks being constructed on-site. The large storage tanks are beneficial as foam concentrate can be pumped rapidly from one source to firefighting vehicles during emergency conditions without the huge demand for replenishment. Consequently, these critical considerations lead to storing firefighting foam concentrate in different storage tanks rather than the original, recommended containers.

The present research work experimentally evaluates and assesses the impact of the aforementioned materials on any performance parameters of AFFF, specifically, foaming ability and foam stability. The study examines the compatibility of mild steel, stainless steel, and HDPE with AFFF concentrate. These are the materials that are commonly used when constructing a storage tank for firefighting foam concentrate, specifically AFFF. This is accomplished by performing several analyses (discussed in Section 2) that evaluate the effect of each material on the AFFF concentrate and, thus, on the performance parameters. In all these analyses, the pure AFFF concentrate is utilized as a benchmark to deduce any vital alterations. In such a manner, it is possible to enhance the properties of these engineering materials based on the heat treatment process, microstructural analysis, and environmental stress cracking in such a way that they are compatible with AFFF concentrate. All these optimization methods

aim to effectively store AFFF concentrate without affecting any of its performance parameters or chemical composition during vital fire accidents.

2 Materials

The experiment was set to investigate the impact of mild steel, stainless steel, and HDPE on the foaming ability and foam stability of AFFF solution using Fourier transform infrared spectroscopy (FTIR), transmission electron microscopy (TEM), dynamic light Scattering (DLS) and inductively coupled plasma atomic emission spectroscopy (ICP-AES).

3 Methodology

Samples of stainless steel, mild steel, and HDPE, together with the AFFF concentrate, were carefully prepared. A guillotine machine was used to cut the material sheets into desired shapes and sizes. All the material sheets were cut to the same sizes and shapes for a fair comparison. A total of three samples were used during the experiments. These sample materials were exposed to natural environmental conditions. All the samples were then immersed and soaked in a 3% proportion of AFFF solution for six months. FTIR, TEM, DLS, and ICP-AES wet analyses were performed on sample materials. This was done to analyze the composition and properties of the AFFF concentrate after being exposed to these materials.

Clean sample materials and AFFF concentrate from the manufacturer were used as benchmarks during the tests, and their properties were compared to those of the exposed material to determine whether any critical changes occurred. All the findings were carefully recorded and analyzed. However, it should be noted that the objective was to analyze the AFFF concentrate, not the materials. The experimental procedure followed for all the samples is presented in the flowchart in Figure 1.

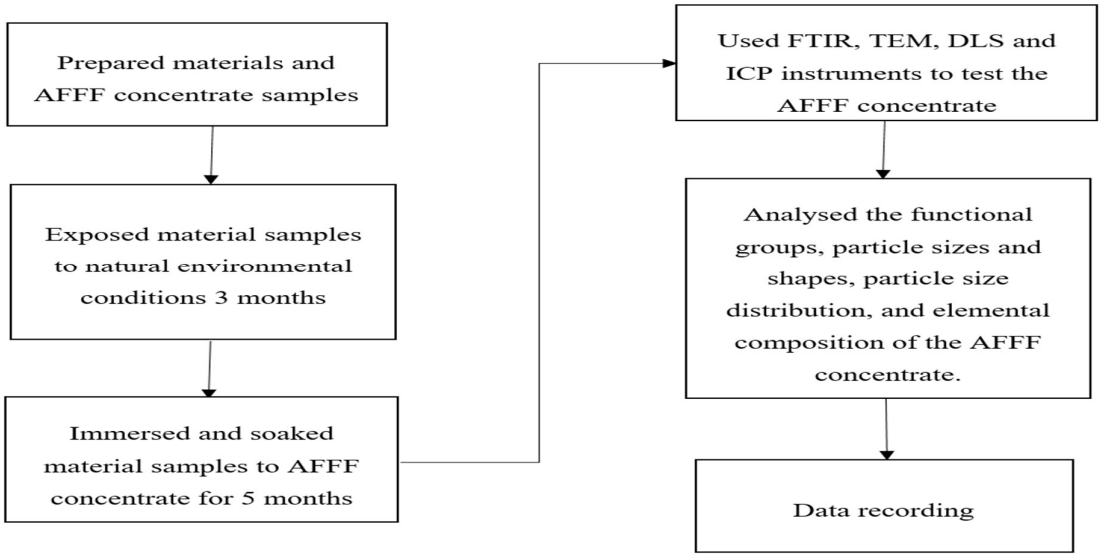

Figure 1: Typical experimental procedure.

4 Materials description

In the present experiments, 3, 4, and 5 mm thick sheets of mild steel, duplex stainless steel, and HDPE, respectively, were selected as the materials of interest. The sample sheets were scribed

to ease the cutting process and ensure that the cut sizes are precise. The cut samples were further cut into three small pieces for accurate testing, and the average results were considered. It was also done to accommodate the percentage errors and external factors that may have occurred during the experimental setup. Glass beakers of 800 ml in volume were prepared to fill the 3% proportion of AFFF concentrate and immerse the material samples. Figures 2 and 3 show the three materials after being cut into desired sizes and immersed in an AFFF concentrate, respectively.

Figure 2: Samples after being cut to desired shapes, mild steel, stainless steel, and HDPE (left to right).

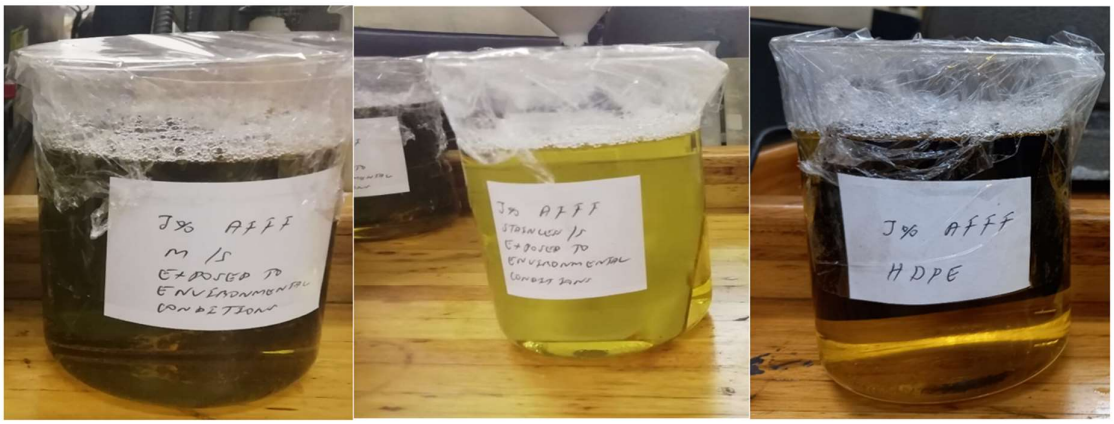

Figure 3: Mild steel, stainless steel, and HDPE (left to right) samples immersed in AFFF. Concentrate.

5 Testing

The various instruments used for distinct experimental analyses are depicted in Figures 4 and 5. These instruments include FTIR, TEM, DLS, and ICP-AES, and their significance in this paper is concisely described under results and discussion in Section 3. All the AFFF samples were analyzed using the FTIR technique. This was accomplished by comparing clean samples from the manufacturer with samples that had been subjected to various material experiments. The FTIR analysis assisted in the identification of functional groups in various exposed samples. Since the FTIR was not able to provide conclusive information, it was essential to validate the FTIR analysis with other tests. TEM analyses were conducted to analyze the large variety of particles, overall particle shape, and visual overall size and shape of the AFFF

concentrate particles using HR imaging and electron diffraction images.

It should be noted that the TEM instrument used does not provide sufficient information on how the particles in the exposed AFFF solution are distributed and does not convey precise particle sizes. However, the DLS instrument was further used to validate the findings of TEM, and it assisted in-depth understanding of the behavior of the AFFF solution particles when exposed to various materials and how their properties were affected. Finally, the ICP-AES test was conducted to identify the chemical elements or composition within the exposed AFFF concentration and benchmark these with the standard qualities. The instruments used during the testing of samples are depicted in Figures 4 and 5.

a) b)

Figure 4: Instruments used during sample testing, FTIR (a) and TEM (b).

a) b)

Figure 5: Instruments used during sample testing, DLS (a) and ICP-AES (b).

6 Results and discussion

7 Infrared spectroscopy of AFFF concentrate

Figure 6 (a-b) shows the FTIR spectra of the pure AFFF concentrate compared to the AFFF concentrate that has been in interaction with the materials of interest. Their functionality in terms of stability, oxidation, and reactivity was revealed. Unsurprisingly, most of the chemical and functional groups appear within the group frequency of wavenumber 4000−1500 cm^{-1}. Referring to Figure 6 (a), it can be observed that at the single bond region, broadband appears at 3355 cm^{-1}, which has been associated with a hydroxy group, H-bonded OH stretch.[9-10] This functional group is responsible for enhancing the ability of AFFF concentrate to dissolve in water.[11] Medial alkyne $C \equiv C$ stretch appears as a weak band at 2120 cm^{-1}, this is a vital distinguishing tool since very few organic compounds reveal an abortion in this region.[9,12] The medium band detected at 1637 cm^{-1} can be assigned to alkenyl $C = C$ stretch vibration.

Interestingly, the fingerprint region also revealed quite a few functional groups. However, the methylene $C-H$ bend and skeletal $C{-}C$ vibrations can be disregarded since they appear in most organic compounds. The fluoro compounds, $C-F$ stretch at 1083 cm^{-1} confirms the presence of fluorosurfactant in AFFF concentrate.

Figure 6 (b) compares the FTIR spectra of a pure AFFF concentrate with an AFFF concentrate that has been in interaction with materials of interest to deduce the significant shifts of functional groups. In the single-bond region, a hydroxy group, H-bonded OH stretch, still appears in all the FTIR spectra. However, there is an unusual absorption peak of aldehyde $C{-}C$ stretching that appears in AFFF solution (HDPE and stainless steel exposed) at bands 2710 cm−1 and 2697 cm^{-1}, respectively.[13] This may indicate an interaction between the AFFF concentrate and two materials (HDPE and stainless steel). Besides, there is a significant shift that can be observed in the triple bond region at bands 2056 and 2060 cm^{-1} for AFFF concentrate when HDPE and stainless steel were immersed, respectively. Consequently, this shift confirms the presence of isothiocyanate $N=C=S$ stretching, which is a very unusual functional group, especially in organic compounds.

It can be clearly observed that there are minor shifts in the functional groups. However, these minor shifts can be subsequently used to predict the reaction of the materials with the AFFF concentrate in the long term. This is a very useful prediction technique since, in the present study, these materials were exposed to AFFF solution for only six months. In addition, the major reaction in the real world may probably take years to occur. Figure 6 (a-c) compares the FTIR spectra of pure materials (HDPE, mild steel, and stainless steel) with materials that were immersed in AFFF concentrate. It was done to further examine and validate the functional group shifts on the exposed materials of interest.

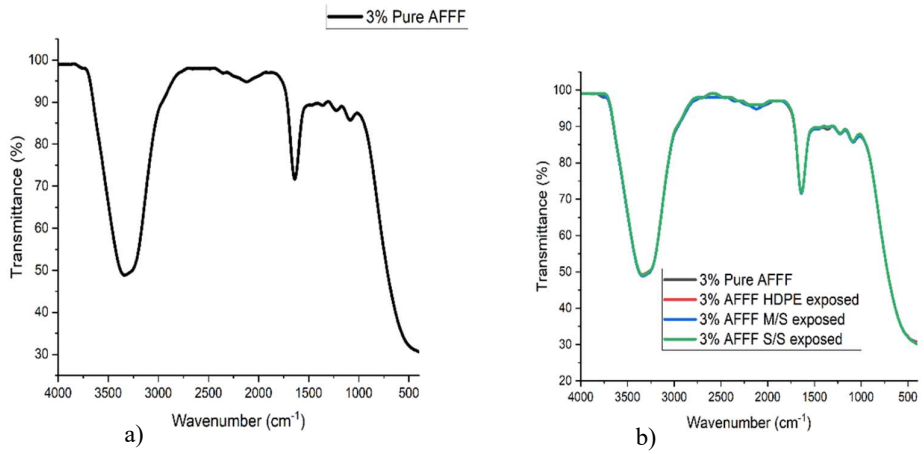

Figure 6: Comparisons of pure AFFF spectra (a) with the other after materials were immersed (b).

8 Infrared spectroscopy of mild steel, stainless steel, and HDPE

The FTIR spectra of the materials of interest were conducted to substantiate the minor shifts of the functional group on the exposed AFFF concentrate. It can be observed from Figure 8 (a-c) that there are significant shifts in functional groups. Referring to Figure 7a, the $O{-}H$ stretching, which can be observed at 3583 cm^{-1} in pure HDPE, shifted to a wavenumber of 3817 cm^{-1} when the materials were immersed in an AFFF concentrate. In pure HDPE, a strong amine N

$-H$ stretching at 3358 cm^{-1} can be seen, which shifts to a broad band at 3406 cm^{-1} in immersed HDPE.

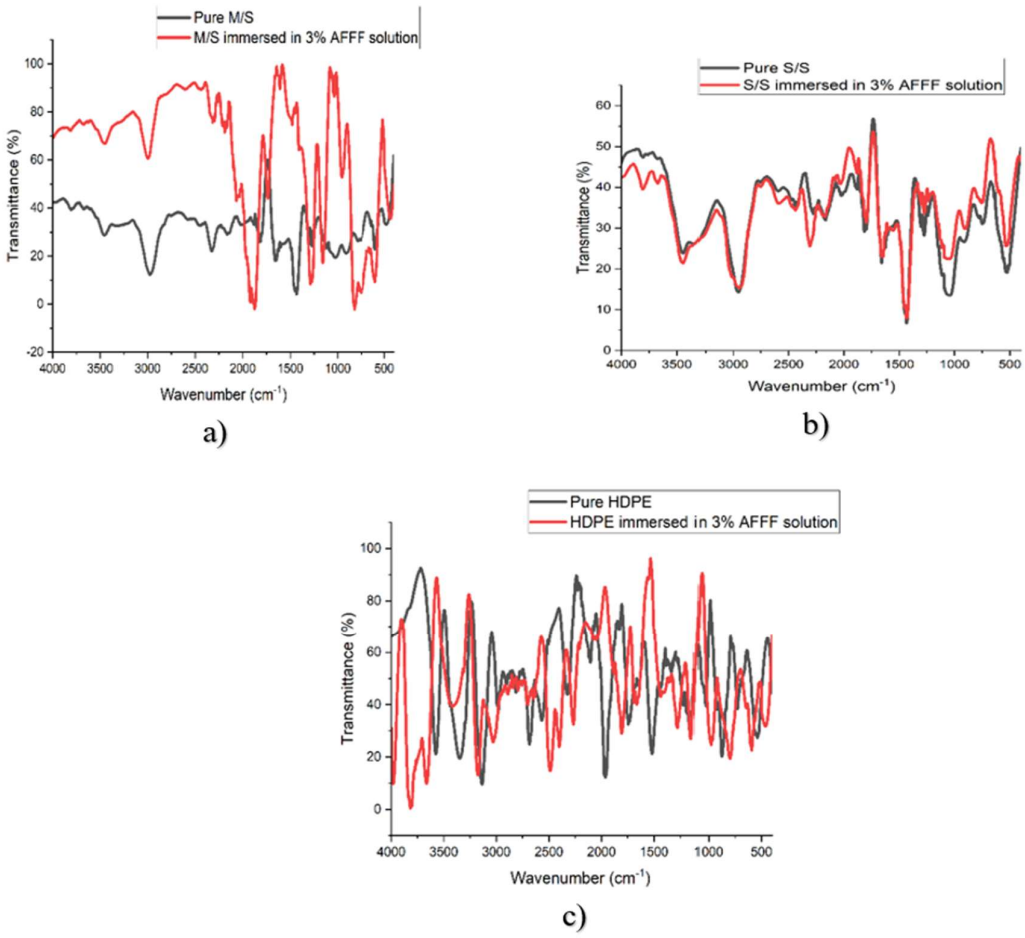

Figure 7: FTIR spectra comparing various materials.

9 Transmission Electron Microscopy (TEM) analyses

The TEM used in this study was able to provide an overall particle shape, a large variety of particles, and a visual overall of the particle shape of the AFFF concentrate samples, using high resolution (HR) and electron diffraction imaging. The TEM images of pure AFFF concentrate are shown in Figure 8 (a-c). These will be utilized as a benchmark and compared to the immersed concentrate to observe critical particle changes. All the samples depict the HR and electron diffraction images in various parts. This was done to understand the overall particle shape of the solution before making any conclusions.

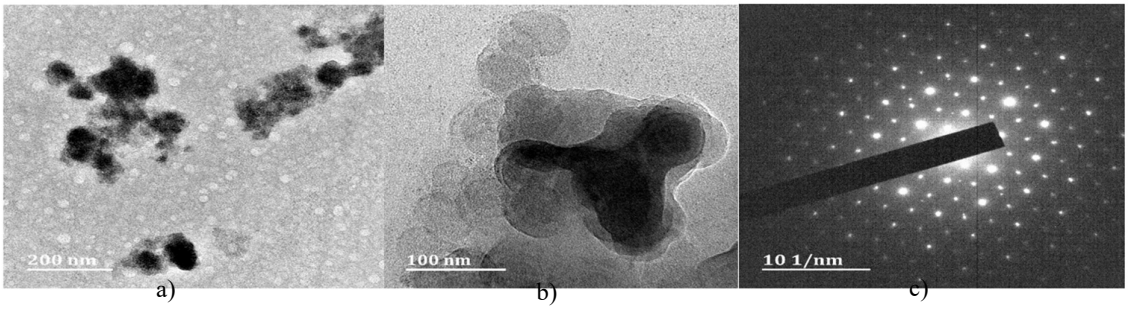

a) b) c)

Figure 8: HR images (a-b) and electron diffraction images (c) of pure AFFF concentrate.

It can be observed from Figure 8 (c) that the electron diffraction image of pure AFFF concentrate provides numerous spots that are aligned in a particular direction. This is a demonstration that the concentrate in a pure state has a single crystalline structure. This shows that the concentrate has uniform properties and is more stable in its pure form.[14-16] Moreover, Figures 8 (a-b) reveal that the particles of pure AFFF concentrate are scattered along the solution. It might be caused by the collision of two or more repelling particles within the solution.[15] Figures 9, 10, and 11 illustrate the HR and electron diffraction images when mild steel, stainless steel, and HDPE, were immersed in AFFF concentrate, respectively.

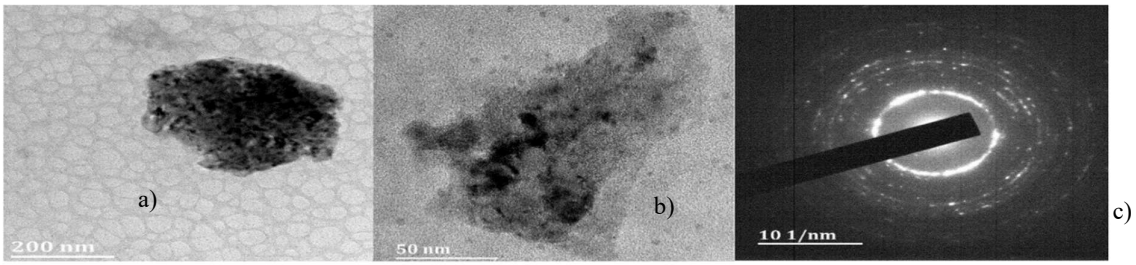

Figure 9: HR images (a-b) and electron diffraction images (c) of AFFF concentrate after mild steel was immersed.

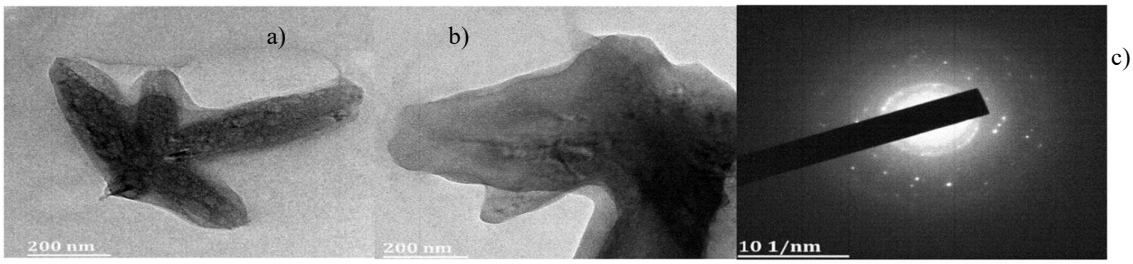

Figure 10: HR images (a-b) and electron diffraction images (c) of AFFF concentrate after stainless steel was immersed.

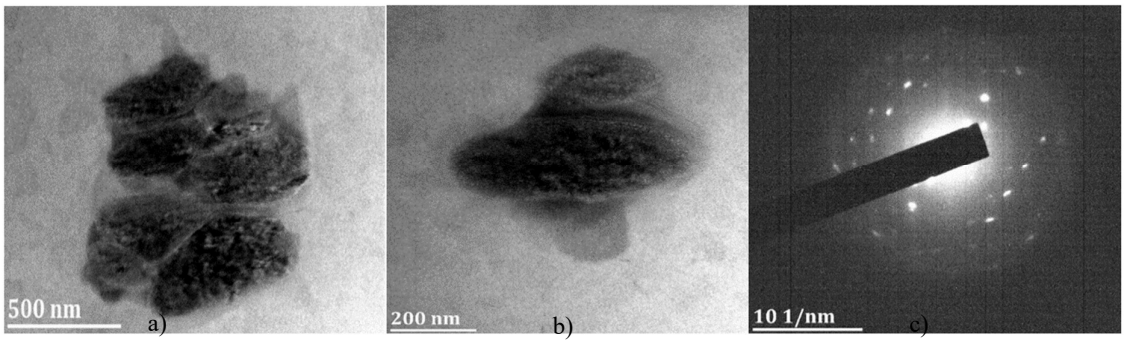

Figure 11: HR images (a-b) and electron diffraction images (c) of AFFF concentrate after HDPE was immersed.

The overall crystal structure and the difference in particle shape for the three samples compared to a pure AFFF sample were studied. Although the present TEM analyses are not able to provide the precise particle sizes of the samples, they nonetheless reveal a significant overall change in the crystal structure. Figure 8 revealed that in a pure state, AFFF concentrate possesses a single crystalline structure. However, when studying Figures 9, 10, and 11 it is observed that the immersed AFFF concentration has critically changed to a polycrystalline.

This is seen in Figures 9 -11 (d) when closely examining the electron diffraction images of these samples. The concentrated circular rounds imply that all these materials are in a polycrystalline state. This is confirmed by the morphology (particles, grains, and crystallites), as several grains are observed in Figures 9, 10, and 11. These grains are separated by grain boundaries and have random crystallographic orientations. It can be further observed that Figure 9 has more grains compared to Figures 10 and 11. Consequently, this implies that most of the crystal structural changes occurred when mild steel was immersed in AFFF concentrate. When comparing the differences topographically (structure and shape), it can be observed in Figure 8 that the particles in a pure AFFF concentration are scattered and distributed along the solution. However, when closely observing Figures 9, 10, and 11 it can be seen that the particles for these samples are concentrated in one area, especially in Figure 9. This demonstrates that when the materials of interest were immersed in the AFFF concentrate, there was a structural and shape particle change. The alteration in crystal structure and particle shape in the AFFF concentrate complements the shifts in functional groups obtained using FTIR. Zhuoqing An et al.[17] experimentally investigated the effect of the particle shape on the viscosity of the liquid. Their results indicated that the spherical particles have a lower viscosity, and any other particle shape will result in higher viscosity. In addition, a change in any additive in the AFFF concentration will affect the foam drainage time. It should be noted that the causes of these alterations are not known as of yet. However, conclusive analyses and interpretation are done in Sections 3.4 and 3.5 using the DLS and elementary analysis to validate the vital information provided by FTIR and TEM.

10 Dynamic Light Scattering (DLS) analyses

An in-depth understanding of the cause of crystal structure and particle shape changes within the AFFF concentrate and the impact these changes possess on the performance parameters are discussed. This is achieved by evaluating the particle size and particle size distribution of the AFFF solution by measuring the hydrodynamic diameter (Z-average) of any present particles in units of nanometres (nm) using a DLS technique. The DLS is a noninvasive technique that depends on the particles moving randomly as a result of collisions with the solvent molecules (Brownian motion). As a result, classification is limited to particles suspended in the liquid.[18] The determination of particle size and size distribution is essential because these characteristics have a significant effect on the properties of the AFFF concentration, including mechanical stability, foaming ability, and viscosity[18].

11 Particle size analysis

Figure 12 depicts the four samples used during the DLS analysis, where samples 1, 2 and 3 are AFFF concentrate when mild steel, stainless steel, and HDPE have been immersed, respectively. Sample 4 is a pure AFFF concentration for benchmark purposes. Also, Table 1 shows the summary of the results for average particle sizes for the four samples in nm.

Figure 12: Samples used during the DLS analysis.

Table 1: Summary of average particle sizes.

SAMPLE ID	Z-AVERAGE [nm]
1	660.7
2	4.892
3	4.036
4	3.586

It can be observed from Table 1 that there have been changes in particle diameter. The pure AFFF concentrate has an average particle size of 3.586 nm, which is a very small particle size. However, when comparing this to samples 2 and 3, it can be observed that there is a slight difference or change. To be precise, the change in Z-average is around 1.306 nm at most. At this point, it is not known if these changes are slight in such a way that they do not have any effect on the properties of the AFFF concentration. Sample 1, in Table 1, shows a major change in particle size. Sample 1 has an average particle size of 660.7 nm, which is way over the other three samples by about 655.808 nm at most. This difference is extremely surprising and has some implications. Larger particles have a slower diffusion speed than smaller particles. In a fluid, a particle's translational diffusion coefficient and hydrodynamic diameter are related by the Stokes-Einstein equation,[19] as shown in equation (1).

$$D_T = \frac{K_b\, T}{b\pi\eta R_h} \tag{1}$$

Where, D_T ($^{m^2}/_{S}$) is the translation diffusion coefficient, RH (m) is the hydrodynamic radius, K_b ($^{J}/_{K}$) is the Boltzmann constant, T is the temperature in Kelvin, η ($^{Ns}/_{m^2}$) is the viscosity of the medium, and b is the constant that depends on the size of the diffusing molecules.

As a matter of fact, for a stable AFFF, rapid diffusion of fluorosurfactant molecules is required.[1] It can be observed from equation (1) that the rate of diffusion is inversely proportional to the particle size. However, it also depends on the surface area and operating temperature. For the present study, all the samples were exposed to the same temperature (atmospheric) for an equitable comparison. This is a demonstration that once the AFFF concentrate has been in contact with mild steel, it decreases its diffusion rate rapidly and thus decreases the foaming ability of the foam solution. On the other hand, the Z-average (particle size diameter) results

demonstrate that when stainless steel and HDPE have been immersed in AFFF concentrate, there are slight differences in particle diameter when compared to pure AFFF solution. When visually observing the numbers, the difference looks slight. On the contrary, the percentage increase calculations demonstrate a relatively large difference, from the fundamental equation given as:

$$\%Increase = \frac{D_s - D_O}{3.586} \times 100 = \frac{4.892 - 3.586}{3.586} \times 100 = 36.419\% \quad (2)$$

It is possible to calculate the percentage increase in particle size for the AFFF concentrate when stainless steel was immersed. where, D_S (nm) is the particle size diameter of sample 2, D_O (nm) is the particle size diameter of sample 4. The same formula employed in equation (2) can be used to calculate the percentage increase in particle size diameter for the AFFF concentration when HDPE was immersed.

$$\%Increase = \frac{D_H - D_O}{3.586} \times 100 = \frac{4.036 - 3.586}{3.586} \times 100 = 12.549\% \quad (3)$$

Where, D_H (nm) is the particle size diameter of the sample. Equation (3) shows that the percentage change in particle size when stainless steel was immersed in an AFFF concentrate was 36.419%. Given that there is a difference of more than a quarter between the two particles, this can be viewed as a significant increase. When examining equation (3), it can be shown that the particle size of HDPE changed on average by 12.549 nm when it was immersed in an AFFF concentrate. With a difference of 23.87 nm, this represents a significantly lower proportion when compared to 36.419 nm. It cannot be guaranteed that it has no impact on an AFFF solution's foaming capabilities, though. At this moment, there are still doubts regarding the effects of these materials on the AFFF concentrate. However, the elemental composition analysis will be carried out in Section 3.4 for additional validation.

12 Particle Size Distribution (PSD) analysis

DLS is a widely accepted method to evaluate the hydro-dynamic size of concentrate particles. The DLS particle size results can be represented using volume, number, and intensity. However, as stated in the international standard (ISO 22412:2017), intensity-based results are the most reliable parameters provided by DLS to describe particle size and particle size distribution (PSD).[19-20] As a consequence, the intensity-based results were opted for in the present research work to analyze the PSD of pure AFFF concentrate and AFFF concentrate after the three materials were immersed.

A comparison in size distribution is then made to understand the influence of each material on the properties of AFFF concentrate. Particle size distribution is essential for understanding the chemical and physical properties of a sample. The particles within the AFFF concentrate have similar sizes and are relatively uniform. The PSD curve of the pure AFFF concentrate plotted by intensity is shown in Figure 13. This PSD curve is used to compare the alteration in PSD of AFFF concentrate when various materials were immersed.

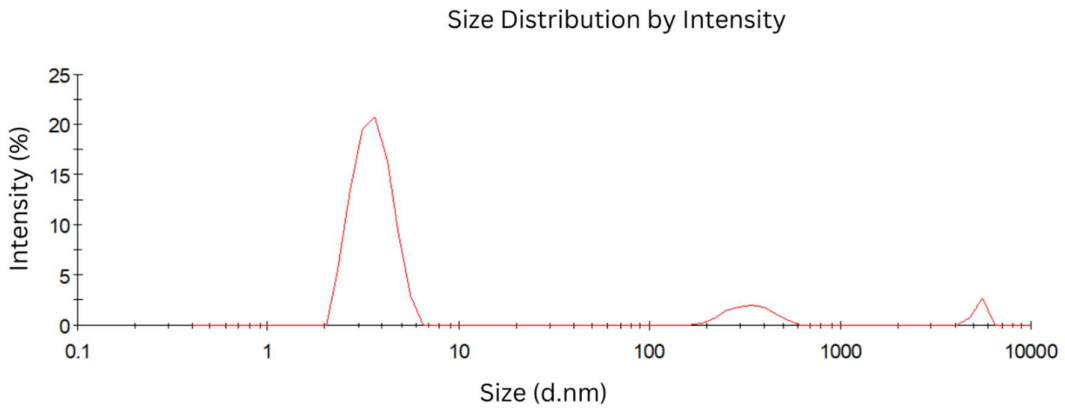

Figure 13: Particle size distribution of pure AFFF concentrate.

It can be observed from Figure 13 that the part size distribution curve shows that the peaks are divided into three intensities. As expected, the major peak is at a particle size of 3.586 nm, as previously shown in Table 1, and the second and third peaks can be estimated at 350 and 5500 nm, respectively. De la Calle et al.[21] studied the particle size distribution of aqueous concentrate. They demonstrated that the aqueous concentrate with a narrow PSD was able to disperse easily. Similarly, it is further seen that the first peak is very narrow. As expected, this is evidence that in a pure state, AFFF concentrate is able to disperse or spread rapidly over a large surface area. precisely the same observation as in Figure 13.

Unsurprisingly, the main peak can be attributed to a particle size of 4.892 nm. Moreover, it can be seen from Figure 14 that the main peak has a narrow PSD. However, when closely observed, it is slightly wider compared to Figure 13. This demonstrates that stainless steel did not cause any critical alteration of PSD within the AFF concentrate, as it is still able to disperse easily. This is a validation that stainless steel does not influence the spreading ability of AFFF. This further concludes that the minor particle size alteration discussed in Section 3.4.1 and Equation (2) does not have a significant impact on the diffusion rate of fluorosurfactant molecules.

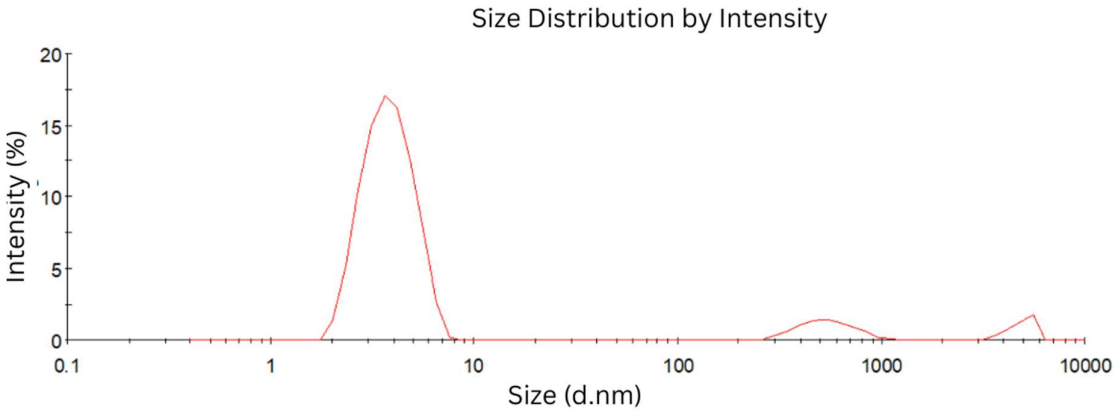

Figure 14: Particle size distribution of AFFF concentrate when stainless steel was immersed.

Referring to Figure 14, it is observed that the AFFF concentrate possesses three peaks. This is precisely the same observation as in Figure 13. Unsurprisingly, the main peak can be attributed

to a particle size of 4.892 nm. Moreover, it can be seen from Figure 14 that the main peak has a narrow PSD. However, when closely observed, it is slightly wider compared to Figure 13. This demonstrates that stainless steel did not cause any critical alteration of PSD within the AFF concentrate, as it is still able to disperse easily. This is a validation that stainless steel does not influence the spreading ability of AFFF. This further concludes that the minor particle size alteration discussed in Section 3.4.1 and Equation (2) does not have a significant impact on the diffusion rate of fluorosurfactant molecules.

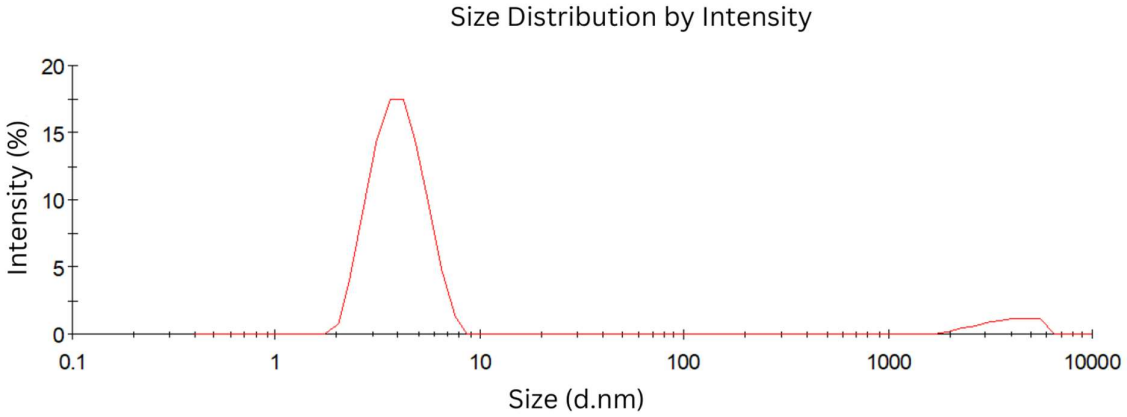

Figure 15: Particle size distribution of AFFF concentrate when HDPE was immersed.

It can be observed from Figure 15 that the PSD curve consists of peaks that are divided into two intensities. This is in contrast to Figures 13 and 14, where the peaks were divided into three intensities. The major peak can be associated with a particle size of 4.036 nm, whereas the other peak can be estimated at 5000 nm. When observing the broadness of the major peak, it can be noticed that it is wider than the peak in Figure 13 and almost the same size as Figure 14. This, however, can be considered a narrow peak. Moreover, this provides sufficient evidence that HDPE does not alter the PSD within the pure AFFF concentrate, which suggests that the dispersion rate is not affected. This further concludes that the minor particle size alteration discussed in Section 3.4.1 and Equation (3) does not have a significant impact on the diffusion rate of fluorosurfactant molecules.

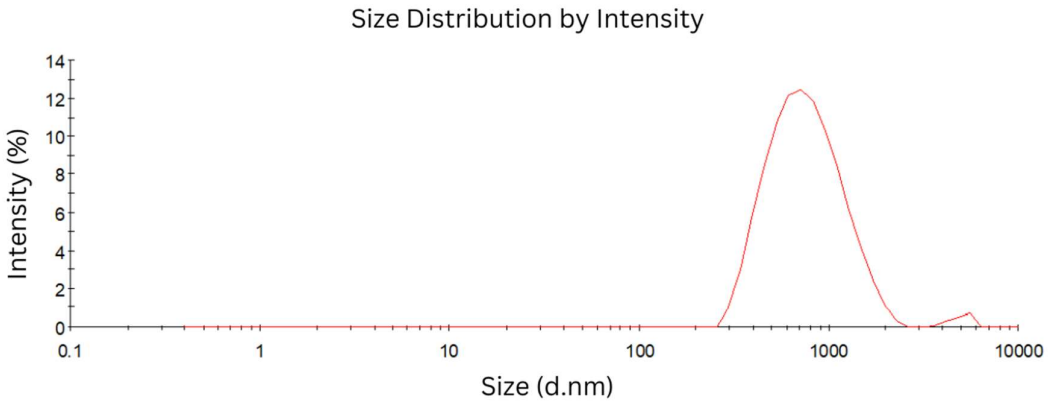

Figure 16: Particle size distribution of AFFF concentrate when mild steel was immersed.

Surprisingly, Figure 16 depicts a distinct PSD compared to Figures 14 and 15. It can be

observed that Figure 16 reveals peaks that are divided into two intensities. These peaks can be associated with particle sizes of 660.7 nm, whereas the other peak can be estimated at 5500 nm. Due to the large difference in sizes between these two peaks, they can be generally regarded as major and minor peaks, respectively. It is interesting to note that Figure 16 possesses a wide major peak compared to all previous peaks illustrated in Figures 13, 14, and 15. This is an indication that there has been a sensitive reaction between mild steel and AFFF concentrate. Moreover, this demonstrates that the spreading ability of the concentrate has been reduced. This could be caused by several parameters, such as an increase in viscosity that causes the concentrate to be slightly thicker. However, it is well known that viscosity is largely dependent on the shape of the particles, where any deviation from the spherical shape of the particle increases viscosity.[22-23] Nevertheless, it is noticed in Figure 16 that the alteration in PSD can have a slight impact on the spreading capability of the aqueous concentrate.

13 Elemental composition analyses

To validate the previous tests conducted using FTIR, TEM, and DLS instruments, the analyses of chemical composition within AFFF concentrate were conducted. The elementary results are more reliable as they provide the precise elements or composition that are present within the AFFF solution before and after the materials were immersed. In this study, the elements of interest were sodium and sulfate. This is because AFFF is water-based and commonly contains a hydrocarbon-based surfactant such as sodium alkyl sulfate. Xiaoyang Yu et al.[24] studied the formation of stable aqueous foams. They experimentally demonstrated that the presence of sodium and Sulfur within the aqueous solution is responsible for the stable foam formation.
As a matter of fact, for stable foam formation, there must be less surface tension in the water. This is mostly accomplished by increasing the sodium alkyl sulfate concentration. Table 2 depicts the elementary results of the pure AFFF concentrate and others when mild steel, stainless steel, and HDPE were immersed. The appendix that contains the entire table of elementary results is available upon request, for validation purposes.

Table 1: Chemical elements of AFFF concentrate.

Element	Chemical symbol	Composition in PPM Sample ID:			
		1	2	3	4
Sodium	Na	2302	2332	2349	2354
Sulfur	S	92	89	94.2	94.7

Referring to Table 2, where samples 1-3 are the AFFF concentrate after mild steel, stainless steel, and HDPE were immersed, respectively, with sample 4 being the pure AFFF concentrate. From Table 2, it can be observed that in a pure state, AFFF concentrate has 2354 and 94.7 parts per million (ppm) of sodium and sulfur, respectively. When observing closely, it is seen that the sodium in pure AFFF concentrate (sample 4) decreases gradually. To be precise, the sodium is reduced by 5, 22, and 52 ppm, respectively, from the pure AFFF concentrate. This indicates that the sodium composition of the AFFF concentrate is reduced when it is exposed to the

materials of interest. Moreover, it can be observed that the amount of sodium is diverse in all samples. This further demonstrates that the severity of the effects caused by the materials on the foam's stability varies greatly.

Similar occurrences can be observed with sulfur (see Table 2). It can be observed that the sulfur composition of pure AFFF concentrate is decreased when it is exposed to various materials. Consequently, this is evident that the reaction of the three materials with the AFFF concentrate reduces the surfactants (sodium alkyl sulfate). This increases the surface tension of water within the solution and thus decreases the stability of the foam. Moreover, it can be seen that the sodium alkyl sulfate was immensely reduced when the AFFF concentration was in contact with mild steel (sample 1). These findings correlate with FTIR, which confirmed the presence of isothiocyanate N=C=S stretching on the triple bond region at bands 2056 cm^{-1} and 2060 cm^{-1}. This is a functional group that confirmed the presence of sulfur in the AFFF concentrate when HDPE and stainless steel were immersed but does not appear in the AFFF concentrate when mild steel was immersed. In addition, the elementary findings further correlate with a gradual diffusion rate of surfactants due to large particles as discussed in Section 3.4.1.

The ICP-AES used for the present research was not able to detect organic compounds. However, the functional groups revealed by FTIR spectra were sufficient to provide the key variations of the elements within the AFFF concentrate. The shifting of the C-F stretch observed in Section 3.1 confirmed that the materials of interest also affect the fluorine content that is present within the PFAS in AFFF concentrate. This alteration of fluorine is a huge setback for the performance parameters of AFFF. PFAS are responsible for forming an aqueous film on fire fuels, which effectively suffocates them by creating a barrier to any oxygen and cooling them to prevent hot fuels from reigniting.[25] Consequently, the alteration of fluorine within the AFFF concentrate greatly reduces the blanketing capabilities during firefighting. It is well known that PFAS are harmful to the environment and humans (carcinogenic). However, the AFFF is primarily chosen for its effective extinguishing capabilities due to PFAS. This implies that any alteration of fluorine within the AFFF concentrate yields unfavorable outcomes. Other vital elements that influence the performance of AFFF are listed in Table 3 and concisely discussed.

Table 2: Chemical elements of AFFF concentrate.

Element	Chemical symbol	Composition in PPM Sample ID:			
		1	2	3	4
Aluminium	Al	0.9	0.2	0.5	1.1
Calcium	Ca	46	07	10	6.9
Iron	Fe	132	58	3.7	2.5
Potassium	K	04	03	2.8	2.4
Magnesium	Mg	27	03	2.4	2.3
Silicon	Si	07	07	11	10.6

Referring to Table 3, it is noticed that the iron content observed in pure AFFF concentrate increased when various materials were immersed. Initially, the iron concentration was 2.5 ppm; it then increased to 3.7 ppm, 58 ppm, and 132 ppm when HDPE, stainless steel, and mild steel were immersed, respectively. In general, the increase in iron predominantly implies the

degradation or wearing of the material.[26] Consequently, this demonstrates that mild steel degrades immensely when in contact with the AFFF concentrate, as the iron element increases by 129.5 ppm. This is evidence that there is a severe reaction between AFFF concentrate and mild steel. The obvious reason for this could be the initiation of corrosion in mild steel when it was first exposed to environmental conditions before immersion in AFFF concentrate. On the other hand, HDPE and stainless steel underwent a similar process, with severity being a major difference. The iron element increased by 1.2 and 55.5 ppm when HDPE and stainless steel reacted with AFFF concentrate, respectively.

The other elements, such as calcium, potassium, and magnesium, are typically water additives. However, the concern is the variation of these elements across the four samples. Subsequently, the degradation of the materials made the AFFF concentrate impure, possibly influencing its firefighting capabilities. This is drawn from visual observation of the various AFFF concentrates during the post-experimental work. Figure 17 depicts the state of pureness of AFFF concentrate after the immersion of materials.

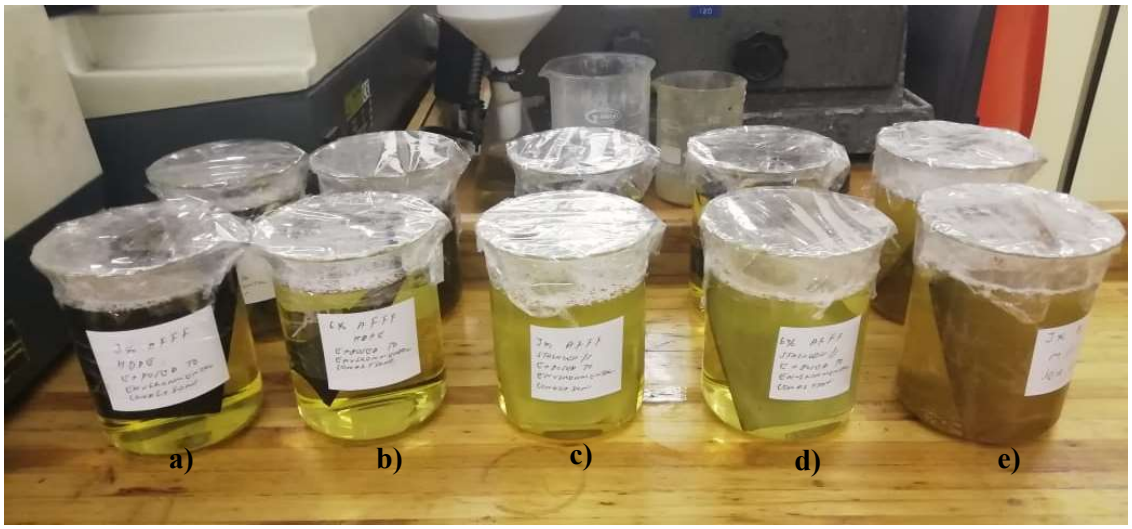

Figure 17: Pureness of AFFF concentrate after immersion of the materials.

It can be observed from Figure 17 that the pureness of the samples varies greatly. Samples (a-b) are AFFF concentrates when HDPE was immersed, and samples (c-d) are when stainless steel was immersed. It is clear from these samples that there was no significant degradation of the materials immersed. This is because the AFFF concentrate was able to maintain its pure yellowish color during the interaction with these materials. However, when observing closely, it is noticed that samples (a–b) are purer than samples (c–d). This is evidence that stainless steel also underwent the degradation process due to the increase of iron by 55.5 ppm, as suggested by Table 3. In contrast, sample (e) is the AFFF concentrate when mild steel was immersed. It can be visually observed that mild steel is immensely degraded when it interacts with AFFF concentrate. The AFFF concentrate's transition from a yellowish to a brownish color serves as visual evidence of this. This is further justified by the large increase in iron of 129.5 ppm observed in Table 3. Although the precise performance parameters affected by this degradation cannot be concluded, the reaction between mild steel and AFFF concentrate remains severe.

14 Conclusions and future work

The main purpose of this research was to investigate the impact of mild steel, stainless steel, and HDPE on the foam ability and foam stability of the AFFF solution. A complete methodology, from sample preparation to testing, was presented. The study was able to experimentally demonstrate that all three materials of interest have a negative impact on the AFFF concentrate with mild steel having a severe impact.

To begin with, this was accomplished by using the FTIR to identify the shifts of the functional groups within the AFFF solution. It was discovered in this study that once mild steel has been in contact with an AFFF concentrate, the isothiocyanate N=C=S functional group could not be detected. On the contrary, the same functional group was identified when stainless steel and HDPE were immersed in the AFFF concentration This is evidence that mild steel influences the chemical compounds of AFFF surfactants, specifically the sodium alkyl sulfate. Consequently, this reaction reduces the foam stability of the AFFF solution during firefighting circumstances.

When the HR imaging provided by TEM was further analyzed, it was discovered that there was a structural and shape particle change when the materials of interest were immersed in the AFFF concentrate. The alteration in crystal structure and particle shape in the AFFF concentrate complements the shifts in functional groups obtained using FTIR. Although TEM did not provide conclusive information, it did show that there is a chemical reaction between the materials and the AFFF concentrate. To underpin the structural and particle shape changes, detailed particle analyses were made using the DLS instrument. It was found that the particle size of the AFFF concentrate had immensely increased when mild steel was immersed. Moreover, when stainless steel and HDPE were immersed, there were minimal alterations within the particle sizes. The analyses demonstrated that the interaction of mild steel with AFFF concentrate causes the gradual diffusion of surfactant (sodium alkyl sulfate) molecules. In fact, AFFF is a low-expansion foam with an expansion ratio of less than 20.[27] This implies that it quickly spreads around a large surface area due to its low viscosity and rapid diffusion rate of surfactants. Consequently, the gradual diffusion of surfactants reduces the spreading capabilities of AFFF during emergency conditions. This is a huge setback as AFFF is normally preferred to extinguish Class B fires due to its rapid spreading rate.

To further underpin that there has been a chemical reaction between the AFFF solution and three materials, the elementary analysis was performed. Although numerous elements were analyzed within the AFFF solution, the interest was in sodium and sulfur, as these are the elements that make up the sodium alkyl sulfate surfactant. The elementary analysis showed that sodium and sulfur are reduced within the AFFF concentrate when it interacts with the materials of interest. The decrease in sodium and sulfur was minimal when the AFFF concentration interacted with stainless steel and HDPE. When mild steel was immersed in the AFFF concentrate, the concentration was extreme (52 PPM). This demonstrated that all three materials affect the stability of AFFF, with the severity of the threat varying.

Based on the findings, it is clear that mild steel is not compatible with the AFFF concentrate. Although it is a relatively cheap option when selecting a storage tank for the AFFF concentrate, some optimization within the material should be made to avoid the degradation of AFFF. The obvious enhancement is the initiation of a relevant heat treatment process that will alter the properties in such a way that it is compatible with AFFF. Stainless steel could be an option as

well, as it has minimal effects on the AFFF. The huge concern is that it is not economical, making it an unfeasible option. As a result, HDPE is a viable option for storing AFFF concentrate. However, it also has the concern of suffering from environmental stress cracking (ESC). This is normally avoided by cross-linking the HDPE to produce cross-linked polyethylene (XLPE). Nonetheless, more research should be conducted to validate its resistance to ESC when in interaction with AFFF concentrate. In addition, plastic materials have the fundamental advantage of being inexpensive. In the 21st century, storage tanks are usually constructed using fiberglass. This material is gradually replacing the material used for constructing the storage tanks due to several benefits, including being chemically resistant.[28] As a consequence, fiberglass is undoubtedly a material to consider when selecting a storage tank for the AFFF concentrate.

The study is limited to the impacts of the three materials on the foaming ability and foam stability of the AFFF solution. Further research work should be conducted to thoroughly investigate other performance parameters of the AFFF that are affected by the interaction of AFFF concentrate with mild steel, stainless steel, and HDPE. In this way, it will be uncomplicated to optimize these materials in such a way that they are compatible with the AFFF concentrate. Moreover, other studies should focus on the possible impacts that fiberglass and cross-linked polyethylene (XLPE) can pose to AFFF concentrate. This will establish several risk-free options for storing AFFF concentrate.

ACKNOWLEDGMENTS

The authors are grateful to National Research Foundation for funding this research work (Grant/Award Number: MND200611530513) and all the laboratories where the experimental work was conducted: Durban University of Technology and the University of Kwa-Zulu Natal.

References

1. Adhikari P. Understanding firefighting foams, Technical Report. Tribhuvan University, 2018. https://www.researchgate.net/publication/324475987.

2. Oguike R. Study of firefighting foam agent from palm oil for extinguishing of petrol fires. *Science Post print* 1 (2013). Doi: 10.14340/spp.2013.12a0002.

3. Dauchy X, Boiteux V, Bach C, Rosin C, Munoz J. Per- and polyfluoroalkyl substances in firefighting foam concentrates and water samples collected near sites impacted by the use of these foams, *Chemosphere* 183 (2017) 53–61. Doi: 10.1016/j.chemosphere.2017.05.056.

4. Scheffey JL, Darwin RL, Leonard JT. Evaluating firefighting foams for aviation fire protection, *Fire Technology* 31 (1995) 224– 243. Doi: 10.1007/BF01039193.

5. Meldrum DN, Williams JR, Conway CJ. Storage life and utility of mechanical fire-fighting foam liquids, *Fire Technology* 1 (1965) 112–121. Doi: 10.1007/BF02588481.

6. Fire service manual. Volume 1. Fire service technology, equipment and media. Communications and mobilizing, HM Fire Service Inspectorate Publication Section, London: The Stationary Office, 2000.

7. Wang S. Research on aqueous film-forming foam concentrate formulations and properties, IOP Conference Series: *Earth and Environmental Science* 295 (2019) 1–4. Doi: 10.1088/1755- 1315/295/3/032072.

8. Rie DH, Lee JW, Kim S. Class b fire-extinguishing performance evaluation of a compressed air foam system at different air-to-aqueous foam solution mixing ratios, *Applied Sciences* 6 (2016) 191. Doi: 10.3390/app6070191.

9. Nandiyanto A, Oktiani R, Ragadhita R. How to read and interpret FTIR spectroscope of organic material, *Indonesian Journal of Science & Technology* 4 (2019) 97–118. Doi:10.17509/ijost.v4i1.15806.

10. Coates JP. The interpretation of infrared spectra: Published reference sources, *Applied Spectroscopy Reviews* 31 (2006) 179–192. Doi:10.1080/05704929608000568.

11. Kovacic J. The c-n stretching in the infrared spectra of Schiff base complexes, *Materials and Process Engineering* 23 (1967) 183–187.

12. Gaffney JS, Marley NA, Jones DE. Fourier Transform Infrared (FTIR) Spectroscopy, *Charact. Mater.* (2012) 1104–1135. doi:10.1002/0471266965. I.A.

13. Mudunkotuwa A, Minshid AL, Grassian VH. ATR-FTIR spectroscopy as a tool to probe surface adsorption on nanoparticles at the liquid-solid interface in environmentally and biologically relevant media, *Analyst*. 139 (2014) 870–81. doi:10.1039/c3an01684f.

14. Bandyopadhyay S. Characterization of metal nanoparticles, New York: McGraw-Hill Education, 1 edition.

15. Pyrz WD, Buttrey DJ. "Particle size determination using TEM: a discussion of image acquisition and analysis for the novice microscopist," *Langmuir 24* (2008) 11350–11360, doi: 10.1021/la801367j.

16. Klein KL, Anderson IM, De Jonge N. "Transmission electron microscopy with a liquid flow cell," *J. Microsc*. 242 (2) (2011) 117–123.

17. Zhuoqing An, Yanling Zhang, Qi Li, Haoran Wang, Zhancheng Guo. Jesse Zhu, Effect of particle shape on the apparent viscosity of liquid–solid suspensions, Powder Technology 328 (2018) 199–206. Doi:10.1016/j.powtec.2017.12.019.

18. Machhi HK, Ray D, Panjabi SH, Aswal VK, Soni SS. "Effect of redox active multivalent metal salts on micellization of amphiphilic block copolymer for energy storage devices via SANS, DLS and NMR," *Molecular Liquids*, vol. 341, pp. 116904, 2021, doi.org/10.1016/j.molliq.2021.116904.

19. Ramirez LMF, Rihouey C, Chaubet F, Le Cerf D, Picton L. "Characterization of dextran particle size: How frit-inlet asymmetrical flow field-flow fractionation (FI-AF4) coupled," *Chromatography A,* vol.1653, pp. 462404, 2021, doi.org/10.1016/j.chroma.2021.462404.

20. Karau A, Benken C, Thömmes J, Kula MR. "The Influence of Particle Size Distribution and Operating Conditions on the Adsorption Performance in Fluidized Beds" *Biotechnology and Bioengineering,* vol. 55, no. 1, pp. 54-64, 2000, doi.org/10.1002/(SICI)1097-0290(19970705)55:1<54::AID-BIT7>3.0.CO;2-W

21. I. De la Calle, Pérez-Rodríguez P, Soto-Gómez D, López-Periago JE. "Detection and characterization of Cu-bearing particles in throughfall samples from vine leaves by DLS, AF4-MALLS (-ICP-MS) and SP-ICP-MS," *Microchemical Journal*, vol.133, pp. 293-301,2017, doi.org/10.1016/j.microc.2017.03.034

22. Koca HD, Doganay S, Turgut A, Tavman IH, Saidur R, Mahbubul IM. "Effect of particle size on the viscosity of nanofluids: A review" *Renewable and Sustainable Energy Reviews,* vol.82, pp. 1664-1674, 2018, doi.org/10.1016/j.rser.2017.07.016.

23. Chantrell R, Popplewell J, Charles S. Measurements of particle size distribution parameters in ferrofluids. IEEE Transactions on Magnetics. 1978 Sep;14(5):975-7.

24. Xiaoyang Yu, Ning Jiang, Xuyang Miao, Ruowen Zong, You- Jie Sheng, Changhai Li, Shouxiang Lu. Formation of stable aqueous foams on the ethanol layer: Synergistic stabilization of fluorosurfactant and polymers, Colloids and Surfaces A: *Physicochemical and Engineering Aspects* 591 (2020) 124545. Doi: 10.1016/j.colsurfa.2020.124545.

25. Zhisheng Xu, Xing Guo, Long Yan, Wendong Kang. Fire- extinguishing performance and mechanism of aqueous film-forming foam in diesel pool fire, *Case Studies in Thermal Engineering* 17 (2019) 100578. Doi: 10.1016/j.csite.2019.100578.

26. Mcarthur H, Spalding D. "Metal and alloys," in *Engineering Materials and Science Properties, Uses, Degradation, Remediation*, Woodhead Publishing Limited, Ed. Cambridge: Horwood Publishing Limited, 2004, pp. 316–363.

27. Mukunda HS, Dixit CSB. Phenomenological model and experimental comparisons on static foam drainage for firefighting foams, Fire Science and Technology 35 (2016) 1–17. Doi: 10.3210/fst.35.1.

28. Avdeeva A, Shlykova I, Perez M, Antonova M, Belyaeva S. "Chemical properties of reinforcing fiberglass in aggressive media," *Engineering and Technology*, vol. 53, 2016, doi:10.1051/matecconf/20165301004.